NIH Public Access
Author Manuscript
J Cell Sci. Author manuscript; available in PMC 2011 December 14.

Published in final edited form as:
J Cell Sci. 2006 June 1; 119(Pt 11): 2258–2268. doi:10.1242/jcs.02953.

N-terminal residues in Cx43 and Cx40 determine physiological properties of gap junction channels, but do not influence heteromeric assembly with each other or with Cx26

Joanna Gemel[1], **Xianming Lin**[2], **Richard D. Veenstra**[2], and **Eric C. Beyer**[1,*]

[1]Department of Pediatrics, Section of Hematology/Oncology and Stem Cell Transplantation, University of Chicago, Chicago MC4060, 5841 S. Maryland Ave, Chicago, IL 60637-1470, USA

[2]Department of Pharmacology, SUNY Upstate Medical University, Syracuse, NY 13210, USA

Summary

The cytoplasmic N-terminal domain in the connexins (Cx) has been implicated in determining several properties including connexin hetero-oligomerization, channel gating and regulation by polyamines. To elucidate the roles of potentially crucial amino acids, we produced site-directed mutants of connexins Cx40 and Cx43 (Cx40E12S,E13G and Cx43D12S,K13G) in which the charged amino acids at positions 12 and 13 were replaced with serine and glycine as found in Cx32. HeLa, N2a and HEK293 cells were transfected and studied by immunochemistry and double whole-cell patch clamping. Immunoblotting confirmed production of the mutant proteins, and immunofluorescence localized them to punctuate distributions along appositional membranes. Cx40E12S,E13G and Cx43D12S,K13G formed homotypic gap junction channels that allowed intercellular passage of Lucifer Yellow and electrical current, but these channels exhibited negligible voltage-dependent gating properties. Unlike wild-type Cx40, Cx40E12S,E13G channels were insensitive to block by 2 mM spermine. Affinity purification of material solubilized by Triton X-100 from cells co-expressing mutant Cx43 or mutant Cx40 with wild-type Cx40, Cx43 or Cx26 showed that introducing the mutations did not affect the compatibility or incompatibility of these proteins for heteromeric mixing. Co-expression of Cx40E12S,E13G with wild-type Cx40 or Cx43 dramatically reduced voltage-dependent gating. Thus, whereas the charged amino acids at positions 12 and 13 of Cx40 or Cx43 are not required for gap junction assembly or the compatibility of oligomerization with each other or with Cx26, they strongly influence several physiological properties including those of heteromeric channels.

Keywords

Intercellular communication; Heteromeric channels; Gap junctions; Connexins; Channel gating

Introduction

Gap junctions are ubiquitous, specialized plasma membrane regions containing intercellular channels. These channels allow passage of low-molecular-weight molecules (ions, metabolites, second messengers and growth regulators) between adjacent cells. A complete, dodecameric, gap junction channel is formed by docking of two hexameric hemichannels (connexons) each comprising subunit proteins called connexins (for reviews, see Harris, 2001; Saez et al., 2003). The connexins span the membrane four times. Their cytoplasmic

*Author for correspondence (ebeyer@peds.bsd.uchicago.edu).

NIH-PA Author Manuscript
NIH-PA Author Manuscript
NIH-PA Author Manuscript

NIH-PA Author Manuscript

NIH-PA Author Manuscript

NIH-PA Author Manuscript

regions (N-terminus, loop between transmembrane domains TM2 and TM3, and C-terminus) exhibit the most sequence variation and might confer connexin-specific properties.

Individual amino acids and domains within the connexin sequences that influence various properties are being identified by expression of differing wild-type connexins or by expression of site-directed mutants and chimeric connexins. All connexins contain a short (≤24 amino acids) cytoplasmic N-terminal region. Charged amino acids within this region influence various physiological properties including transjunctional voltage (V_j)-dependent gating (Verselis et al., 1994; Oh et al., 2000; Purnick et al., 2000b; Musa et al., 2004), unitary conductance (Musa et al., 2004; Tong et al., 2004) and sensitivity to regulation by polyamines (Musa et al., 2004). Lagree et al. have suggested that amino acids 12 and 13 (numbered according to Cx43) also influence the function and compatibility of connexins (Lagree et al., 2003).

Many cells express more than one connexin. Biochemical data have demonstrated the formation of heteromeric channels in several tissues (Jiang and Goodenough, 1996; Bevans et al., 1998; Berthoud et al., 2001), and electrophysiological studies of cultured cells have further supported their existence (Brink et al., 1997; He et al., 1999; Cottrell and Burt, 2001). Co-expression of connexins and heteromeric channel formation might have profound effects on conductance, permeability, selectivity and regulation of gap junction channels. Many of the connexins can be included in groups (α and β) based on sequence similarity (Kumar and Gilula, 1992; Willecke et al., 2002) that also roughly correspond to heteromeric compatibility groups (Yeager and Nicholson, 1996; Kumar, 1999). Our own data are generally consistent with this classification. Using a variety of immunochemical and electrophysiological assays, we have found that Cx43 and Cx37 (Cx43/Cx37) (Brink et al., 1997), Cx43/Cx40 (Valiunas et al., 2001), and Cx43/Cx45 (Martinez et al., 2002) are compatible for heteromeric oligomerization, but Cx43/Cx26 (Gemel et al., 2004) are not.

Amino acid sequence alignments show that the ‘α-group’ of connexins have charged amino acids at positions 12 and 13 whereas, in the ‘β’ connexins, the corresponding amino acids (positions 11 and 12 in Cx26 or Cx32) are uncharged, but polar. Lagree et al. have suggested that these might be crucial amino acids for heteromeric compatibility (Lagree et al., 2003), since replacement of Cx43 residues D12 and K13 with the corresponding amino acids found in Cx32 (S and G, respectively) produced a mutant Cx43 that apparently formed heteromers with Cx32. When co-expressed with a DsRed-tagged Cx32, the Cx43 mutant rescued the trafficking of Cx32-DsRed, since they co-localized at the plasma membrane. Moreover, the mutant acted as a dominant inhibitor of intercellular communication by abolishing transfer of Lucifer Yellow when co-expressed with Cx32.

The experiments described here were designed to examine the importance of these amino acids in the functional behavior and interactions of the connexins that we have previously examined (Cx40, Cx43 and Cx26). We have conducted an immunochemical and physiological analysis of the roles of these amino acids by studying S12,G13 substitution mutants of Cx40 and Cx43.

Results

Expression of Cx40E12S,E13G and Cx43D12S,K13G in transfected cells

To examine the roles of amino acids 12 and 13 in determining the oligomerization and functional properties of Cx40 and Cx43, we transfected communication-deficient HeLa cells with Cx40E12S,E13G or Cx43D12S,K13G. We also produced cell lines co-expressing wild-type and mutant connexins.

NIH-PA Author Manuscript

NIH-PA Author Manuscript

NIH-PA Author Manuscript

Expression of transfected connexin proteins was verified by immunoblotting (Fig. 1). In untransfected HeLa or HEK cells, no immunoreactive Cx40 was detected with anti-Cx40 antibodies (Fig. 1A, lanes 1 and 6, respectively). By contrast, two closely migrating bands (M_r ~38–40 kDa) were observed in HeLa cells transfected with Cx40E12S,E13G or with wild-type Cx40, in cells co-transfected with wild-type Cx40 and Cx43, in cells co-transfected with wild-type Cx40 and Cx43D12S,K13G, and in HEK cells transfected with Cx40E12S,E13G (Fig. 1A). In all cases, the slower-migrating band was more abundant than the faster-migrating band; relative differences might reflect the presence of phosphorylated and unphosphorylated Cx40 forms (Matesic et al., 2003).

In the untransfected HeLa cells, no Cx43 immunoreactivity was observed (Fig. 1B, lane 1). By contrast, multiple Cx43 electrophoretic variants were detected in HeLa cells transfected with wild-type Cx43 or with Cx43D12S,K13G, in cells co-transfected with wild-type Cx40 and Cx43, in cells co-transfected with wild-type Cx40 and Cx43D12S,K13G, in HEK cells, and in HEK cells transfected with Cx40E12S,E13G (Fig. 1B). The HeLa-Cx43 cells and the HeLa-Cx43/Cx40 cells (Fig. 1B) showed a pattern of Cx43 bands similar to that seen in many Cx43-expressing cells (including the HEK cells) resulting from connexin phosphorylation (reviewed by Lampe and Lau, 2004). All cells showed multiple variants. The abundance of slower-migrating Cx43 forms was reduced in cells expressing the connexin mutants (Fig. 1B).

Immunofluorescent staining showed similar distributions of the expressed mutant connexins in HeLa-Cx40E12S,E13G (Fig. 2A) and HeLa-Cx43D12S,K13G (Fig. 2B) cells. Some of the immunoreactive connexin was localized in a punctuate distribution along appositional membranes, and some localized in the cytoplasm. This distribution pattern was similar to that observed for HeLa cells transfected with the corresponding wild-type connexins (Valiunas et al., 2001) and probably represents connexins within gap junction plaques and within the biosynthetic pathway.

Function of Cx40E12S,E13G and Cx43D12S, K13G gap junction channels

To screen for the formation of functional gap junction channels by Cx40E12S,E13G or Cx43D12S,K13G, we microinjected Lucifer Yellow into HeLa cells stably transfected with these mutant connexins. Intercellular transfer of Lucifer Yellow was observed in both HeLa-Cx40E12S,E13G and HeLa-Cx43D12S,K13G cells (Fig. 3A,B). Moreover, dye transfer was also observed in HeLa-Cx40/Cx43D12S,K13G cells (Fig. 3C). The transfer of Lucifer Yellow was quantified by performing multiple injections and counting dye-filled neighbors (Table 1). Whereas some cells expressing wild-type Cx40 alone or together with Cx43 did not always show transfer (69% and 86%, respectively), all injections into cells expressing Cx40E12S,E13G or Cx43D12S,K13G (alone or together with a wild-type connexin) showed transfer. The extent of Lucifer Yellow transfer between HeLa-Cx43D12S,K13G cells was significantly reduced as compared with that between HeLa-Cx43 cells (3.60 versus 8.00 dye-filled neighbors). By contrast, there was no significant difference in dye transfer between HeLa-Cx40E12S,E13G and Hela-Cx40 cells or between HeLa-Cx40/Cx43D12S,K13G and HeLa-Cx40/Cx43 cells. Expression of Cx40E12S,E13G, Cx43D12S,K13G, Cx40E12P,E13G or Cx43D12P,K13G in N2a cells allowed passage of intercellular currents detected by double whole-cell patch clamping (not shown).

Voltage-dependent gating

We compared the voltage-dependent gating (V_j) of the Cx40E12S,E13G and Cx43D12S,K13G gap junction currents to those of wild-type Cx40 or Cx43 (Fig. 4). Wild-type Cx40 and Cx43 gap junction channels exhibited V_j-dependent gating that could be fit with Boltzmann relationships (Fig. 4A,B and Table 2) similar to those previously published

NIH-PA Author Manuscript

NIH-PA Author Manuscript

NIH-PA Author Manuscript

for these connexins (Musa et al., 2004). By contrast, Cx40E12S,E13G and Cx43D12S,K13G showed only a modest reduction of gap junctional conductance at high V_j (Fig. 4C,D). The junctional conductance-voltage (G_j-V_j) relationships for Cx40E12S,E13G and Cx43D12S,K13G could not be fit with a Boltzmann relationship, but did show a linear fit (Fig. 4C,D and Table 3). Cell pairs expressing the proline substitution mutants Cx40E12P,E13G and Cx43D12P,K13G yielded quantitatively similar results to the corresponding serine substitution mutants (data not shown).

Effects on gating polarity can be best characterized by studying one connexin in heterotypic combination with a cell expressing a different connexin. Therefore, we studied cell pairs expressing heterotypic gap junctions formed by wild-type Cx40 or Cx43 paired with their S12,G13 substitution mutants. The heterotypic gap junctions were highly asymmetric, indicating alteration of charges contributing to the voltage sensor for both connexins (Fig. 4E,F and Table 2). At negative V_j relative to the wild-type connexin, voltage-dependent reductions in junctional conductance were limited to 15–20% of the maximum conductance (G_{max}) attained at −25 mV for Cx40 and −50 mV for Cx43. At voltages positive to G_{max}, junctional conductance declined according to a single Boltzmann function with a reduced voltage sensitivity but a lower minimum conductance (G_{min}) relative to the wild-type connexin.

Spermine block in cells expressing Cx40E12S,E13G

To determine if the Cx40E12S,E13G mutations also had a prominent effect on the Cx40 block by spermine, unilateral 2 mM spermine was added in experiments performed using cell pairs expressing homotypic wild-type Cx40 or Cx40E12S,E13G gap junctions (Fig. 5). When V_j was negative relative to the spermine-containing cell, the junctional currents associated with each 10 mV incremental step increased ohmically until voltage gating commenced above −40 mV in the wild-type Cx40 cell pair (Fig. 5A). At positive voltages, junctional current was reduced in a time- and voltage-dependent manner beginning at +20 mV in the wild-type Cx40 experiment, but only slightly at +60 mV in the Cx40E12S,E13G experiment (B). The block at +60 mV was 81±5% (n=3) for wild-type Cx40 gap junctions, but was only 12% for Cx40E12S,E13G.

Single channel properties of SG substitution mutants

We attempted to examine the properties of wild-type and mutant Cx40 and Cx43 channels in low-conductance transfected N2a cell pairs. Wild-type Cx40 and wild-type Cx43 showed discrete long-duration channel openings of ~160 and 100 picoseconds, respectively (Fig. 6, top two traces), as seen in previous analyses (Veenstra et al., 1992; Beblo et al., 1995). By contrast, channel recordings obtained from pairs of cells expressing Cx40E12S,E13G were characterized by very rapid current fluctuations of <100 picoseconds in amplitude (third trace). N2a cells expressing the Cx43D12S,K13G mutant almost uniformly had high conductances, making it very difficult to obtain single channel recordings. However, in one isolated observation, these cells gave an apparent unitary conductance (γ_j) of 30 picoSiemens (not shown).

Effects of SG substitutions on heteromeric compatibility

We used double-label confocal immunofluorescence microscopy to examine the effects of the SG substitutions on the relative localization of the mutants compared with co-expressed wild-type ‘α’ (Cx40 or Cx43) or ‘β’ (Cx26) connexins. In HeLa-Cx40/Cx43D12S,K13G cells, immunoreactive Cx40 and Cx43 showed identical distributions at appositional membranes (Fig. 7A,B) with precise co-localization (Fig. 7C) similar to our previous observations in HeLa cells co-expressing wild-type Cx40 and Cx43 (Valiunas et al., 2001). Similarly, we observed co-localization of transfected Cx40E12S,E13G with wild-type Cx43

NIH-PA Author Manuscript

NIH-PA Author Manuscript

NIH-PA Author Manuscript

in HEK-Cx40E12S,E13G cells (Fig. 7D–F). By contrast, although both Cx43D12S,K13G (Fig. 7G) and Cx26 (Fig. 7H) localized to puncta along appositional membranes in HeLa-Cx26/Cx43D12S,K13G cells, there was little overlap of the two immunoreactivities (Fig. 7I). Some spots showed adjacent red and green, suggesting the presence of both Cx26 and mutant Cx43 (without mixing) in the same gap junction plaques as has been seen with co-expressed wild-type Cx26 and Cx43 (Risek et al., 1994; Falk, 2000; Gemel et al., 2004).

We also used our cells expressing wild-type or mutant Cx43 to examine their localization when co-expressed with Cx32. In HEK293-Cx32 cells, we observed very little overlap of the staining for wild-type Cx32 and Cx43 (Fig. 7J–L). Many plaques contained only Cx32 or Cx43, and there was often separation of the two colors even when they both localized to the same plaque. By contrast, in HeLa-Cx32/Cx43D12S,K13G cells, immunoreactive Cx32 and mutant Cx43 extensively co-localized within the same plaques (Fig. 7M–O). These observations are consistent with the data published by Lagree et al. (Lagree et al., 2003).

The potential heteromeric association of the SG mutants with other connexins was examined using an affinity purification strategy similar to that previously used to study formation of heteromeric connexons between Cx43 and other connexins (Valiunas et al., 2001; Gemel et al., 2004). In each experiment, one of the two co-expressed connexins contained an HA epitope tag. The 100,000 ***g*** supernatant of a 1% Triton X-100 extract was affinity purified using an HA column that allowed binding and elution of the tagged connexin and any tightly associated proteins. Co-elution of a co-expressed connexin suggests heteromeric association (Wang et al., 2005). As expected, wild-type Cx43 co-purified with HA-tagged wild-type Cx40 (Fig. 8A). Similarly, Cx43D12S,K13G co-purified with HA-tagged wild-type Cx40 (Fig. 8B). By contrast, neither wild-type Cx40 or Cx43 nor their mutant counterparts (Cx43D12S,K13G or Cx40E12S,E13G) co-purified with Cx26 (Fig. 8C–F).

Effects of SG substitutions on V_j-dependent gating in co-expressing cells

The ability of the S12,G13 mutant connexins to influence the voltage gating of the wild-type connexins was tested by co-transfecting the mutants into cells expressing wild-type Cx40 or Cx43. Co-expression of Cx40E12S,E13G with wild-type Cx40 nearly abolished voltage-dependent gating (Fig. 9A and Table 2). The steady-state G_j-V_j relationship was strikingly similar to that obtained from pairs of N2a-Cx40E12S,E13G cells (Fig. 4C). By contrast, when Cx43D12S,K13G was co-expressed with wild-type Cx40, significant voltage gating was retained (Fig. 9B and Table 2). There was a significant reduction in the gating charge from approximately 3 to 1 relative to the wild-type Cx40 G_j-V_j curve with only slight increases in the G_{min} or half inactivation voltage ($V_{1/2}$), suggesting some interactions between Cx43D12S,K13G and wild-type Cx40 subunits. Cells co-expressing Cx40E12S,E13G and wild-type Cx43 also exhibited little V_j-dependent gating and yielded a linear G_j-V_j relationship (Fig. 9C and Table 3) that closely resembled that observed in homotypic homomeric N2a-Cx40E12S,E13G cell pairs (Fig. 4C). Co-expression of Cx43D12S,K13G with wild-type Cx43 produced mixed results with different experiments exhibiting minimal, intermediate, or maximal effects on transjunctional voltage-dependent gating properties (Fig. 9D). These diverse observations could result from variable levels of relative wild-type and mutant Cx43 expression.

Spermine effects in co-expressing cells

Treatment of cells co-expressing Cx40E12S,E13G and wild-type Cx40 with 2 mM spermine produced similar results to the homotypic Cx40E12S,E13G experiment, resulting in a 25±9% (n=9) decrease in g_j at +60 mV (Fig. 5C). Whereas the time dependence of the block was similar to that of the mutant Cx40 gap junctions, the slight increase in the amount of block (relative to the mutant expressed by itself) might indicate the presence of some

NIH-PA Author Manuscript

NIH-PA Author Manuscript

NIH-PA Author Manuscript

homomeric wild-type Cx40 gap junction channels. Co-expression of Cx43D12S,K13G with wild-type Cx40 (Fig. 5D) produced only a modest reduction in the amount of block to 26±13% (n=3) at +60 mV (consistent with dilution of the sensitive subunits), with an exponential time course similar to that observed for wild-type Cx40 gap junctions.

Single channels in co-expressing cells

Double whole-cell patch clamp recordings from low-conductance pairs of cells co-expressing wild-type Cx40 and Cx43 (produced by transient transfection of N2a-Cx43 cells with Cx40) showed long duration events with amplitudes consistent with those produced by homomeric wild-type Cx40 and Cx43 (Fig. 6, fourth trace). By contrast, pairs of cells co-expressing Cx40E12S,E13G and wild-type Cx43 produced rapidly fluctuating single channel data similar to that obtained from Cx40E12S,E13G (Fig. 6, bottom trace). Similar 'noisy' current records were also obtained from cells co-expressing wild-type Cx40 and Cx40E12S,E13G (data not shown).

Discussion

In this study, we have presented data showing the consequences of substituting the polar residues serine and glycine (as found in Cx32) for the charged residues found at positions 12 and 13 of Cx40 (E, E) or Cx43 (D, K). In transfected cells, these substitution mutants produced immunoreactive connexins of similar abundance and electrophoretic mobility to their wild-type counterparts and localized appropriately to appositional membranes as expected for gap junction proteins. Our data and those of Lagree et al. (Lagree et al., 2003) suggest that the identity of amino acids 12 and 13 is not crucial for connexin biosynthesis, oligomerization or assembly into gap junction plaques.

In our study, the S12,G13 substitution mutants retained function as detected by dye transfer and electrical coupling. We did not detect any difference in the functional efficiency of the Cx40 mutant as compared with its wild-type counterpart. However, the HeLa-Cx43D12S,K13G cells showed a significant reduction in the extent of Lucifer Yellow transfer (the number of dye-filled neighbors was reduced by 55%), suggesting that Cx43D12S,K13G might have a reduced permeability to this dye as compared with wild-type Cx43. By contrast, Lagree et al. have previously reported that introducing the S and G substitutions into Cx43 abolished Lucifer Yellow transfer (Lagree et al., 2003). However, the two sets of observations might not be inconsistent, since reduced permeability might have reduced dye transfer to undetectable levels in the studies of Lagree et al. (Lagree et al., 2003). There are some methodological differences between the two studies. Lagree et al. used 0.3% Lucifer Yellow, whereas we used 4%. They expressed GFP-tagged connexins whereas ours were unmodified. Connexin chimeras with fluorescent proteins have been extensively used for previous studies of gap junction channel physiology; although most properties are not altered, some chimeras have shown changes in gating (Bukauskas et al., 2001) or passage of large tracers (Beltramello et al., 2003).

Introduction of the S,G substitutions did substantially change the electrophysiological properties of homomeric gap junction channels formed from these connexins. Both Cx40E12S,E13G and Cx43D12S,K13G channels were nearly devoid of V_j-sensitive gating properties, exhibiting only slight linear reductions in G_j with increasing V_j. This result is similar to our previous observations with a charge reversal substitution in Cx40 (substitution of K for E13) that dramatically altered all channel V_j-dependent gating (Musa et al., 2004). The Cx43D12S,K13G data contrast with our previous observation that a K13E mutation in Cx43 did not eliminate V_j-dependent gating (Musa et al., 2004) and suggests the importance of position 12 in Cx43. Taken together, these two studies indicate that these amino acids in the middle of the connexin N-terminal domain are involved in the V_j-dependent gating of

NIH-PA Author Manuscript

NIH-PA Author Manuscript

NIH-PA Author Manuscript

Cx40 and Cx43 gap junction channels. Purnick et al. observed that a S11D substitution (at the corresponding position) in Cx32 shifted the steady-state heterotypic Cx32S11D/Cx32 G_j-V_j relationship, but did not reverse the V_j gating polarity of Cx32 gap junctions, leading them to conclude that this residue is the first residue in the N-terminus to lie outside the V_j field (Purnick et al., 2000b).

The Cx40E12S,E13G substitution mutant showed two altered properties that were similar to our previous observations with a charge reversal mutant (Cx40E13K) at position 13 (Musa et al., 2004). Both Cx40E12S,E13G and Cx40E13K produced 'flickery' channels, and they were minimally sensitive to block by spermine. This suggests that the negative charge at position 13 is crucial for stable channel openings and spermine block, since these properties are disrupted by replacement with either oppositely charged or neutral amino acids.

Purnick et al. used nuclear magnetic resonance analysis of a synthetic peptide corresponding to the N-terminal sequence of Cx26 to develop a model for the structure of this region of the connexins (Purnick et al., 2000a). Their model suggests that the SG motif might form a flexible hinge at the midpoint of the N-terminal domain. Lagree et al. suggested that these amino acids might similarly form a hinge structure when incorporated into the corresponding positions Cx43 (and by our extrapolations, Cx40) (Lagree et al., 2003). Since proline and glycine residues are very common within β-turn structures (Richardson, 1981; Williams et al., 1987), we made P12,G13 substitution mutants of Cx40 and Cx43 and these behaved very similarly to the S12,G13 mutations.

We used double-label confocal immunofluorescence microscopy and an affinity purification technique to assess the potential effects of introducing the S12,G13 substitutions in Cx40 or Cx43 on their ability to oligomerize with each other and Cx26. We did not see any apparent alterations. We found near-perfect co-localization of both connexins in HeLa-Cx40/Cx43D12S,K13G cells and in HEK-Cx40E12S,E13G cells, but little precise co-localization in HeLa-Cx26/Cx43D12S,K13G cells. These results are similar to our observations with co-expressed wild-type Cx40 and Cx43 (Valiunas et al., 2001) or Cx26 and Cx43 (Gemel et al., 2004). By contrast, we confirmed the earlier observations of Lagree et al. that co-expressed wild-type Cx32 and Cx43 do not co-localize, but Cx32 extensively co-localizes with co-expressed Cx43D12S,K13G (Lagree et al., 2003). Our affinity purification experiments using material solubilized with Triton X-100 (containing connexons) consistently showed co-purification of mutant and wild-type forms of Cx40 and Cx43, but did not show co-purification of Cx26 with any forms of Cx40 or Cx43. Our data support the previous conclusion that these residues contribute to the compatibility between Cx32 and Cx43 (Lagree et al., 2003), but we have now shown that it cannot be extended to all other combinations between members of the 'α' and 'β' groups of connexins. Our observations support the suggestion that residues in other connexin domains also influence hetero-oligomerization compatibility, since the mutated Cx40 and Cx43 were not made compatible with Cx26. Lagree et al. have concluded that a residue in the third transmembrane domain is also important for heteromeric mixing (Lagree et al., 2003). Moreover, Maza et al. have identified a motif in this region that prevents Cx43 oligomerization in the endoplasmic reticulum (ER) (Maza et al., 2005); it might prevent hetero-oligomerization of connexins that oligomerize in the ER with those that oligomerize in a later compartment.

In contrast to the biochemical data, our electrophysiological analyses suggest that the S12,G13 substitutions did influence the functional interactions of Cx40 and Cx43. When wild-type Cx40 and wild-type Cx43 were co-expressed, we observed unitary gap junction channel behavior that could be explained by distinct homomeric gap junction channel populations (Fig. 6, fourth traces). (Although heteromeric interactions might occur between these wild-type connexins, they were not needed to explain the physiological data.) These

NIH-PA Author Manuscript

NIH-PA Author Manuscript

NIH-PA Author Manuscript

data are similar to the previous study of Valiunas et al. (Valiunas et al., 2001), but they contrast with the suggestions of other authors that co-expressed Cx40 and Cx43 produce some channels of intermediate sizes (He et al., 1999; Cottrell and Burt, 2001). As we have previously discussed (Valiunas et al., 2001), the Triton X-100 solubilization and subsequent affinity purification and the double whole-cell patch clamp analysis might not examine the same pools of connexins and might produce contrasting results. Double-label immunofluorescence and affinity purification techniques do not allow us to determine stoichiometries of co-expressed connexins in individual channels in plaques. We believe that Cx40 and Cx43 are capable of hetero-oligomerizing within channels, but the fraction of those channels that are functional or are present in the gap junctions might be reduced compared with the homomeric channels or to the extent of heteromerization seen with some other connexin combinations.

Co-expression of Cx40E12S,E13G and wild-type Cx40 yielded physiological results consistent with heteromeric mixing of the two proteins; Cx40E12S,E13G co-expression had a uniformly dominant-negative effect on wild-type Cx40 function, producing a flickery channel and abolishing V_j-dependent gating and spermine block. A more surprising observation was that co-expression of Cx40E12S,E13G had a similar dominant-negative effect on channel function and V_j-dependent gating of wild-type Cx43 gap junctions.

In contrast to the mutant Cx40 protein, co-expression of Cx43D12S,K13G did not produce a complete dominant-negative effect on the V_j-dependent gating of wild-type Cx43 or Cx40 gap junctions. The observations with co-expressed Cx43D12S,K13G and wild-type Cx40 were consistent with parallel spermine-sensitive and insensitive junctional conductances, suggesting incomplete heteromerization of the mutant with wild-type Cx40. The co-expression results with wild-type Cx43 were quite variable; they suggested that the amount of V_j-dependent gating varied based on differing levels of Cx43D12S,K13G expression added to a background of wild-type Cx43 expression.

Taken together, our data suggest that positions 12 and 13 in the connexin NT domain are very important for multiple physiological properties of Cx40 and Cx43 when expressed alone or together. Moreover, our findings might have pathophysiological significance, since several inherited diseases including deafness, keratoses and Charcot-Marie-Tooth disease have been associated with mutations of Cx26, Cx30.3, Cx31 and Cx32 at residues corresponding to those that we have studied (Ressot et al., 1998; Grifa et al., 1999; Richard et al., 2003; Rouan et al., 2003; Essenfelder et al., 2004).

Materials and Methods

Connexin-expressing cells

N2a, HeLa and HEK293 cells were cultured as described previously (Veenstra et al., 1992; Gemel et al., 2004). Generation of N2a or HeLa cells stably expressing rat Cx40 or rat Cx43 have been previously described (Veenstra et al., 1992; Valiunas et al., 2001; Musa et al., 2004).

Mutants of rat Cx40 or rat Cx43 containing substitutions of serine and glycine for amino acids 12 and 13 (Cx40E12S,E13G and Cx43D12S,K13G) or substitutions of proline and glycine (Cx40E12P,E13G and Cx43D12P,K13G) were generated using PCR. Sequences were fully verified by automated sequencing. Connexin DNAs were subcloned into pTracer-CMV2 (Invitrogen) and pcDNA3.1/+ (Invitrogen), using the Xi-clone™ Vector Conversion Kit (Gene Therapy Systems). The plasmid constructs were purified using the High Purity Plasmid Purification Kit (Marligen Biosciences).

NIH-PA Author Manuscript

NIH-PA Author Manuscript

NIH-PA Author Manuscript

Cells expressing individual mutant connexins were generated by stable transfection with linearized pcDNA3.1-connexin DNA using lipofectamine (Invitrogen) and clonal selection in medium containing 500 μg/ml (for HeLa cells) or 400 μg/ml (for HEK293 cells) G418 (Invitrogen).

Clones of cells that stably expressed both Cx40 and Cx43D12S,K13G were generated by transfection of hygromycin-resistant HeLa-Cx40 cells (Valiunas et al., 2001) with Cx43D12S,K13G. Generation of HeLa cells co-expressing Cx40 and Cx43 were described earlier (Valiunas et al., 2001). Cells that stably expressed both Cx43 and Cx40E12S,E13G were generated by transfection of HEK293 cells (which endogenously contain Cx43 protein and channels) with Cx40E12S,E13G and selection with G418. Cells that stably expressed both Cx43 and Cx32 were generated by transfection of HEK293 cells with Cx32 and selection with G418. Cells that expressed both Cx43D12S,K13G and Cx32 were generated by transient transfection of Cx32 into stably transfected HeLa-Cx43D12S,K13G cells. Cells that stably expressed both Cx26 and Cx43D12S,K13G or Cx40E12S,E13G were generated by transfection of puromycin-resistant HeLa-Cx26 cells (Elfgang et al., 1995) (kindly provided by B. Nicholson, University of Texas Health Science Center, San Antonio, TX) with the pcDNA3.1-connexin DNAs and selection with G418.

Stable transfectants were maintained in medium supplemented with the selecting agent at 50% of the concentration used for initial cloning: G418 (250 μg/ml for HeLa cells and 200 μg/ml for HEK293 cells), hygromycin (75 μg/ml), puromycin (0.5 μg/ml). Alternatively, for many of the electrophysiological experiments, N2a or HeLa cells were transiently transfected with connexin DNA in pTracer-CMV2, and transfected cells were identified by GFP fluorescence.

Immunoblot analysis

Immunoblots were performed essentially as described earlier (Elenes et al., 2001). Protein samples (10–20 μg) were resolved on 10% polyacrylamide gels containing sodium dodecyl sulfate (SDS-PAGE). Rainbow molecular mass marker standards (Amersham Biosciences) were used to calibrate the gels. Proteins were electro-transferred from gels onto Immobilon-P membranes (Millipore). Immunoblots were developed with ECL chemiluminescence reagents (Amersham Biosciences).

Antibodies used for connexin detection

Cx43 was detected using a mouse monoclonal antibody (mAb) directed against amino acids 252–270 (Chemicon, MAB 3068) at 1:250 dilution for immunofluorescence or using rabbit polyclonal antibodies directed against amino acids 363–382 of human/rat Cx43 (Sigma, C6219) at 1:4000 for immunoblotting or 1:1000 for immunofluorescence. Cx26 was detected using a mouse mAb directed against a segment of its cytoplasmic loop (Invitrogen/Zymed, 13–8100) at 1:500 dilution for immunoblotting or at 1:250 for immunofluorescence. HA-tagged Cx26 was detected using rabbit anti-HA antibodies (Invitrogen/Zymed, 71–5500) at 1:3000 dilution. A rabbit antiserum directed against a bacterially expressed fusion protein containing the Cx40 C-tail was used for immunoblotting at 1:5000 dilution (Kwong et al., 1998). For immunofluorescence, a rabbit polyclonal antibody directed against a 19 amino acid peptide sequence within the C-terminal cytoplasmic domain of mouse Cx40 (Chemicon AB1726) was used at 1:1000 dilution. To detect Cx32 by immunofluorescence a rabbit antiserum directed against a peptide corresponding to a portion of the cytoplasmic loop of rat Cx32 (Invitrogen/Zymed, 71-0600) was used at 1:250 dilution.

NIH-PA Author Manuscript

NIH-PA Author Manuscript

NIH-PA Author Manuscript

Immunofluorescent labeling of cells

Cells cultured on multiwell slides were stained as described earlier (Gemel et al., 2004) except for fixation with 4% paraformaldehyde for 30 minutes at room temperature. To increase the adherence of HEK293 cells, they were plated on slides coated for 30 minutes with 0.01% poly L-lysine (Sigma).

Affinity purification of HA-tagged proteins

For studies of potential connexin co-purification, one (untagged) connexin was expressed stably, whereas a second (HA-tagged) connexin was introduced by transient transfection. 72 hours following transfection, connexins and connexons were solubilized in 1% Triton X-100 (Berthoud et al., 2001). Samples were centrifuged at 100,000 ***g*** for 30 minutes, and the supernatant (containing solubilized connexons) was affinity purified using the μMACS HA isolation kit (Miltenyi Biotec) with several modifications (Wang et al., 2005). Triton-extracted samples containing 250 μg protein were incubated for 30 minutes at 4°C with 50 μl Anti-Tag MicroBeads in 50 mM Tris-HCl buffer (pH 8.0) containing 150 mM NaCl and 1% Triton X-100. Beads with bound proteins were transferred to columns, placed in the magnetic field, and washed four times with 200 μl of the same buffer. A fifth wash was performed using 100 μl of buffer containing no salt. Bound proteins were eluted with 50 μl of hot (95°C) SDS gel sample buffer. Samples were analyzed by immunoblotting.

Microinjection of gap junction tracers

Cells cultured on coverslips (80–100% confluent) were impaled with a micropipette filled with 150 mmol/l LiCl, 4% Lucifer Yellow (charge = −2, molecular weight = 457; Sigma). The dye solution was microinjected with a picospritzer (model PLI-188, Nikon) using 0.2- to 0.3-second pulses of 1–2 psi. Cells were photographed after 1 minute.

Electrophysiological recordings

The bath saline contained: 142 mM NaCl, 1.3 mM KCl, 0.8 mM $MgSO_4$, 0.9 mM NaH_2PO_4, 1.8 mM $CaCl_2$, 4.0 mM CsCl, 2.0 mM TEACl, 5.5 mM dextrose, 10 mM HEPES, pH 7.4 (titrated with 1N NaOH), and was 310 milliosmolar (mOsm). The standard KCl internal pipette solution contained: 140 mM KCl, 4.0 mM CsCl, 2.0 mM TEACl, 3.0 mM $CaCl_2$, 5.0 mM K_4BAPTA, 1.0 mM $MgCl_2$, 25 mM HEPES, pH 7.4 (titrated with 1N KOH), and was 310 mOsm. MgATP was added daily to achieve a final concentration of 3.0 mM (Veenstra, 2001). All experiments were performed at room temperature (20–22°C) on the stage of an inverted phase contrast microscope (Olympus IMT-2). Junctional current (I_j) recordings were obtained using conventional double whole-cell recording techniques with two Biologic RK-400 (Molecular Kinetics) patch clamp amplifiers. All transjunctional voltage (V_j) errors resulting from the patch electrode series resistance (R_{el}) were corrected during the junctional conductance (g_j) calculations according to the expression (Veenstra, 2001):

$$g_j = \frac{-\Delta I_2}{V_1 - (I_1 \bullet R_{el1}) - V_2 + (I_2 \bullet R_{el2})}.$$

The maximum g_j ($g_{j,max}$) was determined from the linear regression fit of the steady-state I_j-V_j curve from each experiment between ±5 and ±20 mV. Normalized g_j (G_j) was calculated from the ratio of $g_j/g_{j,max}$ for each V_j polarity and normalized $I_j = G_j \times V_j$ for each experiment. For heterotypic gap junctions, g_j was normalized to $g_{j,max}$ from +5 to +20 mV for Cx40 and −20 to −5 mV for Cx43. All normalized I_j and G_j data represent the mean values from 4–6 (n) experiments. All currents were digitized at 1–4 kHz after low pass filtering at 100–500

NIH-PA Author Manuscript

NIH-PA Author Manuscript

NIH-PA Author Manuscript

Hz (LPF 202A; Warner Instruments, Hamden, CT). Curve-fitting procedures were performed using Clampfit software (pClamp version 8.2; Axon Instruments) using the sum of squared errors minimization procedure and the standard error for each estimated parameter is provided. Final graphs were prepared using Origin version 6.1 or 7.0 software (Origin Lab Corporation).

The voltage dependence of the wild-type Cx40 and Cx43 gap junctions was determined in stably transfected N2a cell clones that had been transiently transfected with the pTracer-CMV2 vector (containing no insert) as a control.

Ionic blockade experiments

Spermine HCl_4 (Calbiochem) was stored at −20°C as a 500 mM stock solution in 18 MΩ-cm water and diluted daily as required with KCl IPS. The IPS osmolarity after the addition of 2 mM spermine was altered by at most 3% (Musa and Veenstra, 2003). The magnitude of polyamine block was determined by dividing $-\Delta I_2$ ($=I_j$) during a positive ΔV_1 voltage clamp step by $-\Delta I_2$ obtained during negative ΔV_1 voltage clamp steps of the same magnitude with 2 mM spermine added unilaterally to cell 1.

Acknowledgments

We acknowledge the contributions of A. Martinez for instruction regarding dye injections and B. Goc for technical assistance. This work was supported by NIH grant HL59199 and the Bernice Meltzer Pediatric Cancer Research funds.

References

Beblo DA, Wang HZ, Beyer EC, Westphale EM, Veenstra RD. Unique conductance, gating, and selective permeability properties of gap junction channels formed by connexin40. Circ. Res. 1995; 77:813–822. [PubMed: 7554128]

Beltramello M, Bicego M, Piazza V, Ciubotaru CD, Mammano F, D'Andrea P. Permeability and gating properties of human connexins 26 and 30 expressed in HeLa cells. Biochem. Biophys. Res. Commun. 2003; 305:1024–1033. [PubMed: 12767933]

Berthoud VM, Montegna EA, Atal N, Aithal NH, Brink PR, Beyer EC. Heteromeric connexons formed by the lens connexins, connexin43 and connexin56. Eur. J. Cell Biol. 2001; 80:11–19. [PubMed: 11211930]

Bevans CG, Kordel M, Rhee SK, Harris AL. Isoform composition of connexin channels determines selectivity among second messengers and uncharged molecules. J. Biol. Chem. 1998; 273:2808–2816. [PubMed: 9446589]

Brink PR, Cronin K, Banach K, Peterson E, Westphale EM, Seul KH, Ramanan SV, Beyer EC. Evidence for heteromeric gap junction channels formed from rat connexin43 and human connexin37. Am. J. Physiol. Cell Physiol. 1997; 273:C1386–C1396.

Bukauskas FF, Bukauskiene A, Bennett MV, Verselis VK. Gating properties of gap junction channels assembled from connexin43 and connexin43 fused with green fluorescent protein. Biophys. J. 2001; 81:137–152. [PubMed: 11423402]

Cottrell GT, Burt JM. Heterotypic gap junction channel formation between heteromeric and homomeric Cx40 and Cx43 connexons. Am. J. Physiol. Cell Physiol. 2001; 281:C1559–C1567. [PubMed: 11600419]

Elenes S, Martinez AD, Delmar M, Beyer EC, Moreno AP. Heterotypic docking of Cx43 and Cx45 connexons blocks fast voltage gating of Cx43. Biophys. J. 2001; 81:1406–1418. [PubMed: 11509355]

Elfgang C, Eckert R, Lichtenberg-Frate H, Butterweck A, Traub O, Klein RA, Hulser DF, Willecke K. Specific permeability and selective formation of gap junction channels in connexin-transfected HeLa cells. J. Cell Biol. 1995; 129:805–817. [PubMed: 7537274]

NIH-PA Author Manuscript

NIH-PA Author Manuscript

NIH-PA Author Manuscript

Essenfelder GM, Bruzzone R, Lamartine J, Charollais A, Blanchet-Bardon C, Barbe MT, Meda P, Waksman G. Connexin30 mutations responsible for hidrotic ectodermal dysplasia cause abnormal hemichannel activity. Hum. Mol. Genet. 2004; 13:1703–1714. [PubMed: 15213106]

Falk MM. Connexin-specific distribution within gap junctions revealed in living cells. J. Cell Sci. 2000; 113:4109–4120. [PubMed: 11058097]

Gemel J, Valiunas V, Brink PR, Beyer EC. Connexin43 and connexin26 form gap junctions, but not heteromeric channels in co-expressing cells. J. Cell Sci. 2004; 117:2469–2480. [PubMed: 15128867]

Grifa A, Wagner CA, D'Ambrosio L, Melchionda S, Bernardi F, Lopez-Bigas N, Rabionet R, Arbones M, Monica MD, Estivill X, et al. Mutations in GJB6 cause nonsyndromic autosomal dominant deafness at DFNA3 locus. Nat. Genet. 1999; 23:16–18. [PubMed: 10471490]

Harris AL. Emerging issues of connexin channels: biophysics fills the gap. Q. Rev. Biophys. 2001; 34:325–472. [PubMed: 11838236]

He DS, Jiang JX, Taffet SM, Burt JM. Formation of heteromeric gap junction channels by connexins 40 and 43 in vascular smooth muscle cells. Proc. Natl. Acad. Sci. USA. 1999; 96:6495–6500. [PubMed: 10339616]

Jiang JX, Goodenough DA. Heteromeric connexons in lens gap junction channels. Proc. Natl. Acad. Sci. USA. 1996; 93:1287–1291. [PubMed: 8577756]

Kumar NM. Molecular biology of the interactions between connexins. Novartis Found. Symp. 1999; 219:6–16. [PubMed: 10207895]

Kumar NM, Gilula NB. Molecular biology and genetics of gap junction channels. Semin. Cell Biol. 1992; 3:3–16. [PubMed: 1320430]

Kwong KF, Schuessler RB, Green KG, Laing JG, Beyer EC, Boineau JP, Saffitz JE. Differential expression of gap junction proteins in the canine sinus node. Circ. Res. 1998; 82:604–612. [PubMed: 9529165]

Lagree V, Brunschwig K, Lopez P, Gilula NB, Richard G, Falk MM. Specific amino-acid residues in the N-terminus and TM3 implicated in channel function and oligomerization compatibility of connexin43. J. Cell Sci. 2003; 116:3189–3201. [PubMed: 12829738]

Lampe PD, Lau AF. The effects of connexin phosphorylation on gap junctional communication. Int. J. Biochem. Cell Biol. 2004; 36:1171–1186. [PubMed: 15109565]

Martinez AD, Hayrapetyan V, Moreno AP, Beyer EC. Connexin43 and connexin45 form heteromeric gap junction channels in which individual components determine permeability and regulation. Circ. Res. 2002; 90:1100–1107. [PubMed: 12039800]

Matesic D, Tillen T, Sitaramayya A. Connexin 40 expression in bovine and rat retinas. Cell Biol. Int. 2003; 27:89–99. [PubMed: 12662966]

Maza J, Das Sarma J, Koval M. Defining a minimal motif required to prevent connexin oligomerization in the endoplasmic reticulum. J. Biol. Chem. 2005; 280:21115–21121. [PubMed: 15817491]

Musa H, Veenstra RD. Voltage-dependent blockade of connexin40 gap junctions by spermine. Biophys. J. 2003; 84:205–219. [PubMed: 12524276]

Musa H, Fenn E, Crye M, Gemel J, Beyer EC, Veenstra RD. Amino terminal glutamate residues confer spermine sensitivity and affect voltage gating and channel conductance of rat connexin40 gap junctions. J. Physiol. 2004; 557:863–878. [PubMed: 15107469]

Oh S, Abrams CK, Verselis VK, Bargiello TA. Stoichiometry of transjunctional voltage-gating polarity reversal by a negative charge substitution in the amino terminus of a connexin32 chimera. J. Gen. Physiol. 2000; 116:13–32. [PubMed: 10871637]

Purnick PE, Benjamin DC, Verselis VK, Bargiello TA, Dowd TL. Structure of the amino terminus of a gap junction protein. Arch. Biochem. Biophys. 2000a; 381:181–190. [PubMed: 11032405]

Purnick PE, Oh S, Abrams CK, Verselis VK, Bargiello TA. Reversal of the gating polarity of gap junctions by negative charge substitutions in the N-terminus of connexin 32. Biophys. J. 2000b; 79:2403–2415. [In Process Citation]. [PubMed: 11053119]

Ressot C, Gomes D, Dautigny A, Pham-Dinh D, Bruzzone R. Connexin32 mutations associated with X-linked Charcot-Marie-Tooth disease show two distinct behaviors: loss of function and altered gating properties. J. Neurosci. 1998; 18:4063–4075. [PubMed: 9592087]

NIH-PA Author Manuscript

NIH-PA Author Manuscript

NIH-PA Author Manuscript

Richard G, Brown N, Rouan F, Van der Schroeff JG, Bijlsma E, Eichenfield LE, Sybert VP, Greer KE, Hogan P, Campanelli C, et al. Genetic heterogeneity in erythrokeratodermia variabilis: novel mutations in the connexin gene GJB4 (Cx30.3) and genotype-phenotype correlations. J. Invest. Dermatol. 2003; 120:601–609. [PubMed: 12648223]

Richardson JS. The anatomy and taxonomy of protein structure. Adv. Protein Chem. 1981; 34:167–339. [PubMed: 7020376]

Risek B, Klier FG, Gilula NB. Developmental regulation and structural organization of connexins in epidermal gap junctions. Dev. Biol. 1994; 164:183–196. [PubMed: 8026622]

Rouan F, Lo CW, Fertala A, Wahl M, Jost M, Rodeck U, Uitto J, Richard G. Divergent effects of two sequence variants of GJB3 (G12D and R32W) on the function of connexin 31 in vitro. Exp. Dermatol. 2003; 12:191–197. [PubMed: 12702148]

Saez JC, Berthoud VM, Branes MC, Martinez AD, Beyer EC. Plasma membrane channels formed by connexins: their regulation and functions. Physiol. Rev. 2003; 83:1359–1400. [PubMed: 14506308]

Tong JJ, Liu X, Dong L, Ebihara L. Exchange of gating properties between rat cx46 and chicken cx45.6. Biophys. J. 2004; 87:2397–2406. [PubMed: 15454438]

Valiunas V, Gemel J, Brink PR, Beyer EC. Gap junction channels formed by coexpressed connexin40 and connexin43. Am. J. Physiol. Heart Circ. Physiol. 2001; 281:H1675–H1689. [PubMed: 11557558]

Veenstra RD. Determining ionic permeabilities of gap junction channels. Methods Mol. Biol. 2001; 154:293–311. [PubMed: 11218654]

Veenstra RD, Wang HZ, Westphale EM, Beyer EC. Multiple connexins confer distinct regulatory and conductance properties of gap junctions in developing heart. Circ. Res. 1992; 71:1277–1283. [PubMed: 1382884]

Verselis VK, Ginter CS, Bargiello TA. Opposite voltage gating polarities of two closely related connexins. Nature. 1994; 368:348–351. [PubMed: 8127371]

Wang M, Martinez AD, Berthoud VM, Seul KH, Gemel J, Valiunas V, Kumari S, Brink PR, Beyer EC. Connexin43 with a cytoplasmic loop deletion inhibits the function of several connexins. Biochem. Biophys. Res. Commun. 2005; 333:1185–1193. [PubMed: 15979566]

Willecke K, Eiberger J, Degen J, Eckardt D, Romualdi A, Guldenagel M, Deutsch U, Sohl G. Structural and functional diversity of connexin genes in the mouse and human genome. Biol. Chem. 2002; 383:725–737. [PubMed: 12108537]

Williams RW, Chang A, Juretic S, Loughran D. Secondary structure predictions and medium range interactions. Biochim. Biophys. Acta. 1987; 916:200–204. [PubMed: 3676331]

Yeager M, Nicholson BJ. Structure of gap junction intercellular channels. Curr. Opin. Struct. Biol. 1996; 6:183–192. [PubMed: 8728651]

NIH-PA Author Manuscript
NIH-PA Author Manuscript
NIH-PA Author Manuscript

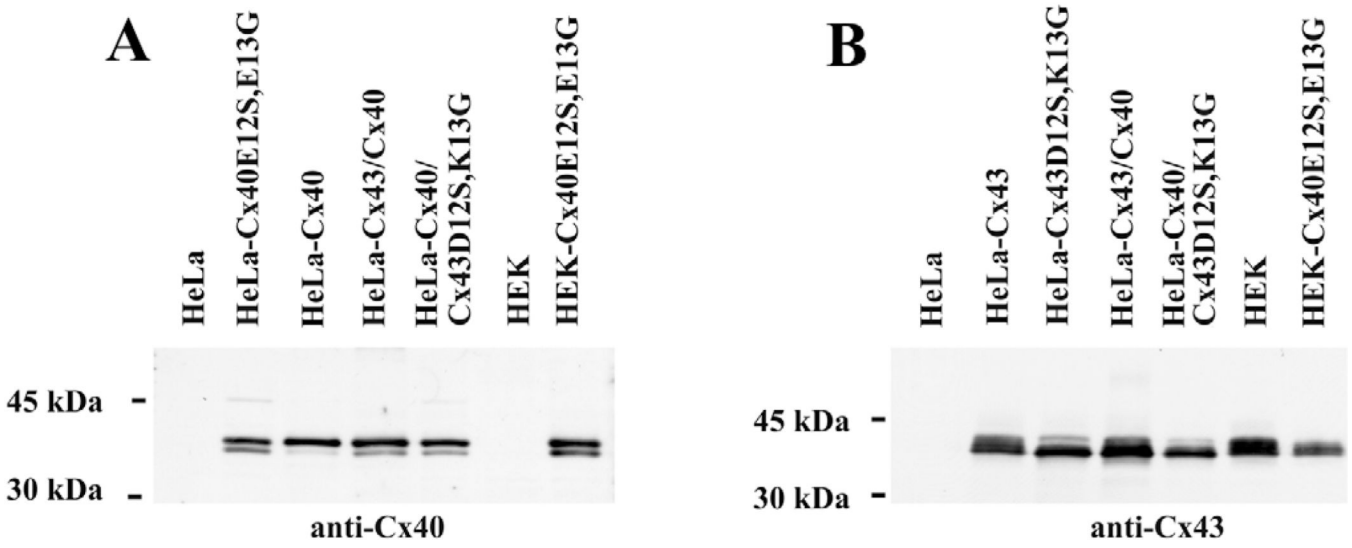

Fig. 1.

Immunoblot detection of Cx40 and Cx43 expression in untransfected and stably transfected HeLa and HEK cells. Whole-cell lysates (10 μg protein for HeLa cells, 20 μg protein for HEK cells in Fig. 1A; 10 μg protein for all samples in Fig. 1B) were resolved by SDS-PAGE, transferred to membranes and blotted with (A) anti-Cx40 or (B) anti-Cx43 antibodies. Migration of molecular weight markers is indicated to the left of the blots.

NIH-PA Author Manuscript
NIH-PA Author Manuscript
NIH-PA Author Manuscript

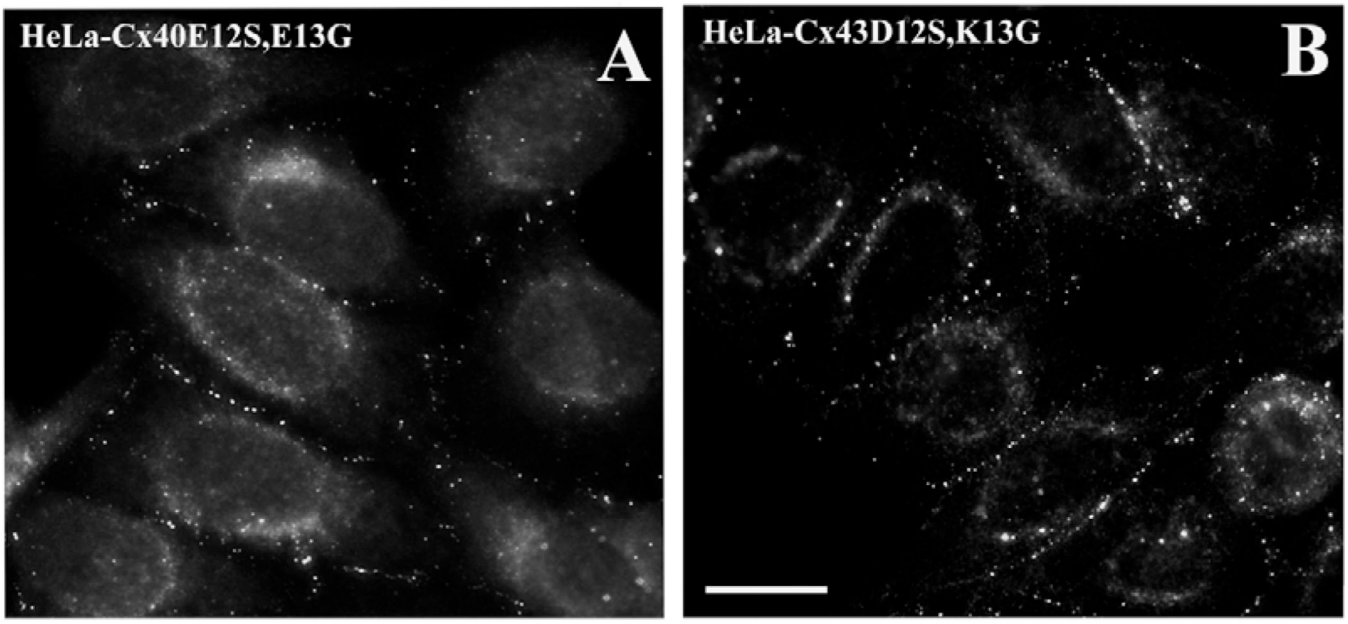

Fig. 2.

Immunofluorescent detection of the distributions of immunoreactive Cx40 (A) in stably transfected HeLa-Cx40E12S,E13G cells and Cx43 (B) in stably transfected HeLa-Cx43D12S,K13G cells. Bar, 20 μm.

NIH-PA Author Manuscript
NIH-PA Author Manuscript
NIH-PA Author Manuscript

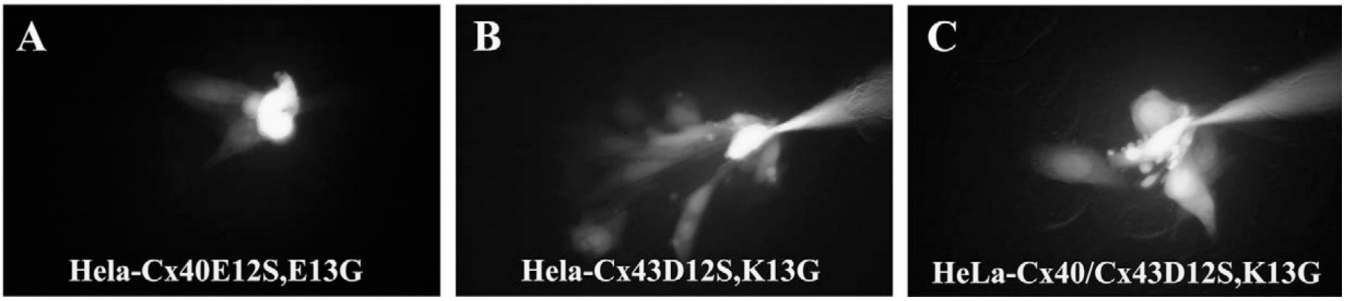

Fig. 3.

Intercellular transfer of microinjected Lucifer Yellow between stably transfected (A) HeLa-Cx40E12S,E13G cells, (B) HeLa-Cx43D12S,K13G cells, and (C) HeLa-Cx40/Cx43D12S,K13G cells.

NIH-PA Author Manuscript
NIH-PA Author Manuscript
NIH-PA Author Manuscript

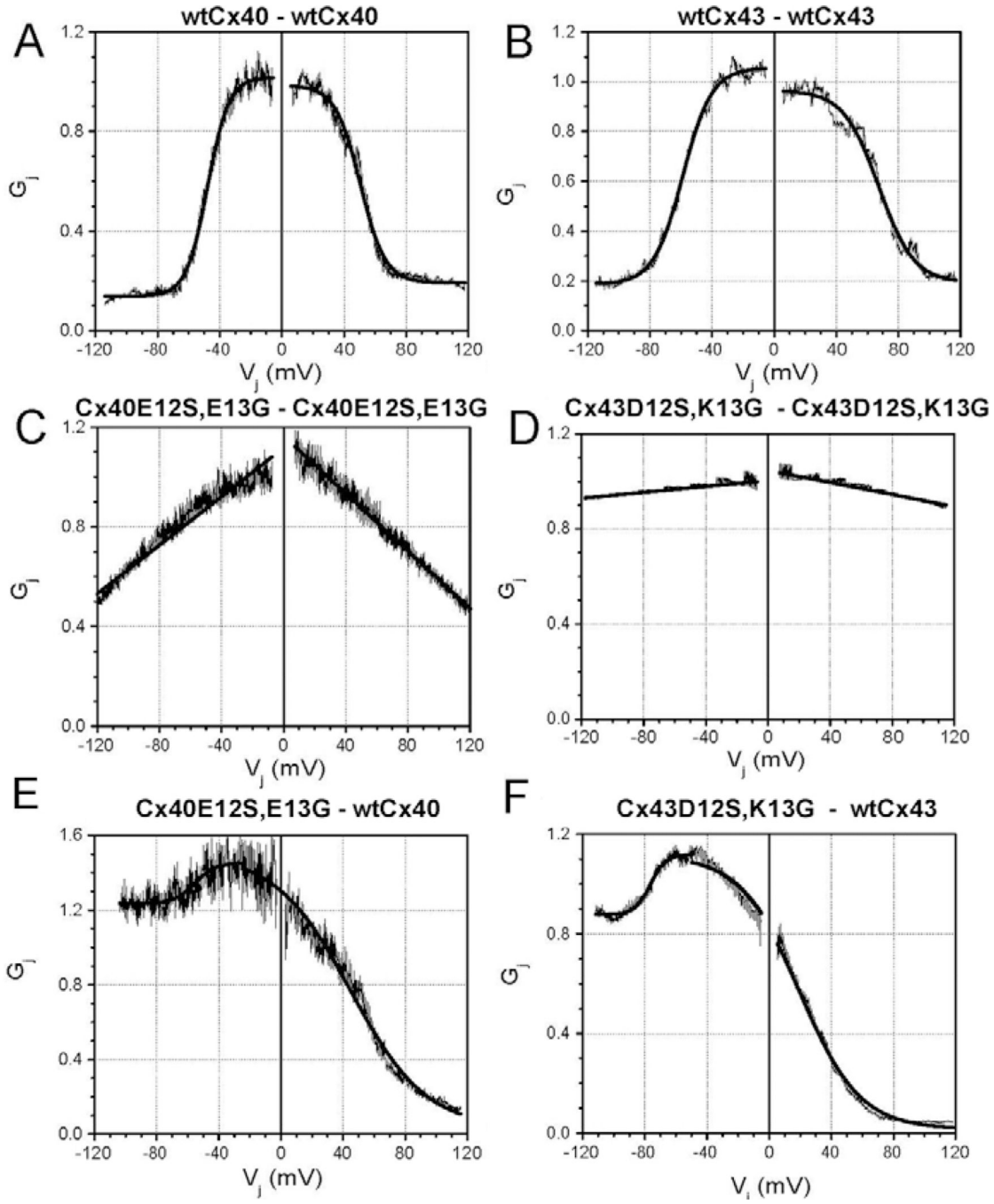

Fig. 4.

Voltage-dependent gating of wild-type (wt) and mutant connexin channels expressed in N2a (A–E) or in HeLa (F) cells. The relationships between normalized steady-state conductance (G_j) and transjunctional voltage (V_j) are shown for cell pairs expressing (A) wtCx40 (stably)-wtCx40 (stably), (B) wtCx43 (stably)-wtCx43 (stably), (C) Cx40E12S,E13G (transiently)-Cx40E12S,E13G (transiently), (D) Cx43D12S,K13G (transiently)-Cx43D12S,K13G (transiently), (E) the heterotypic combination Cx40E12S,E13G (transiently)-wtCx40 (stably), and (F) the heterotypic combination Cx43D12S,K13G (transiently)-wtCx43 (stably). The mathematical fits to the G_j-V_j relationships are described in Tables 2 and 3. All normalized data represent the mean values from 4–6 experiments.

NIH-PA Author Manuscript
NIH-PA Author Manuscript
NIH-PA Author Manuscript

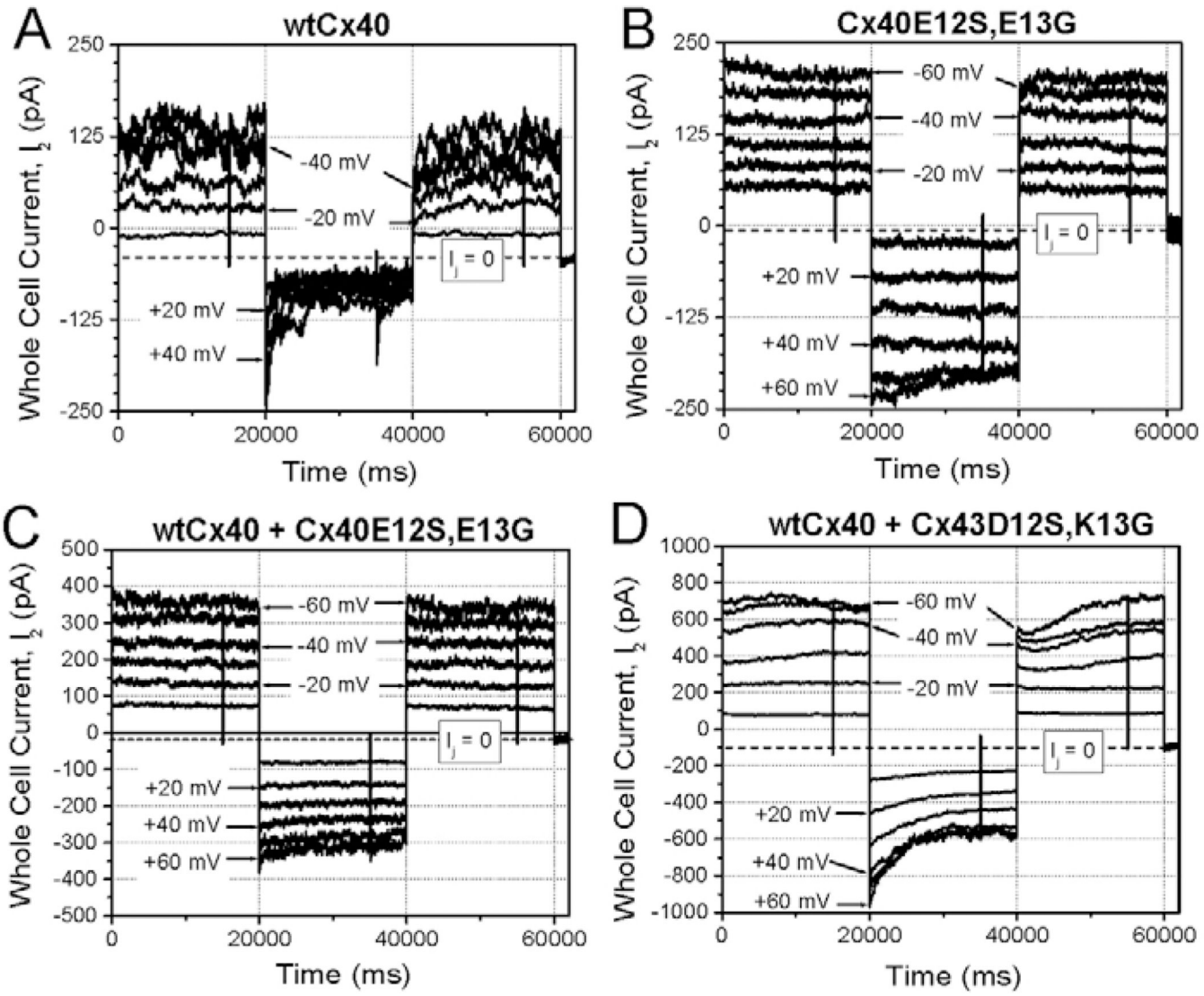

Fig. 5.

Spermine blockade of gap junctional currents in N2a cells expressing wild-type (wt) or mutant Cx40. 2 mM spermine was applied unilaterally (in one pipet) during recording of a family of junctional currents. (A) Currents between a pair of cells (stably) expressing wtCx40 were blocked when V_j was positive (center). (B) Currents between a pair of cells (transiently) expressing Cx40E12S,E13G were not affected by 2 mM spermine. (C) Currents between a pair of cells co-expressing wtCx40 (stably) and Cx40E12S,E13G (transiently) were not affected by 2 mM spermine. (D) Currents between a pair of cells co-expressing wtCx40 (stably) and Cx43D12S,K13G (transiently) were slightly affected by 2 mM spermine.

NIH-PA Author Manuscript

NIH-PA Author Manuscript

NIH-PA Author Manuscript

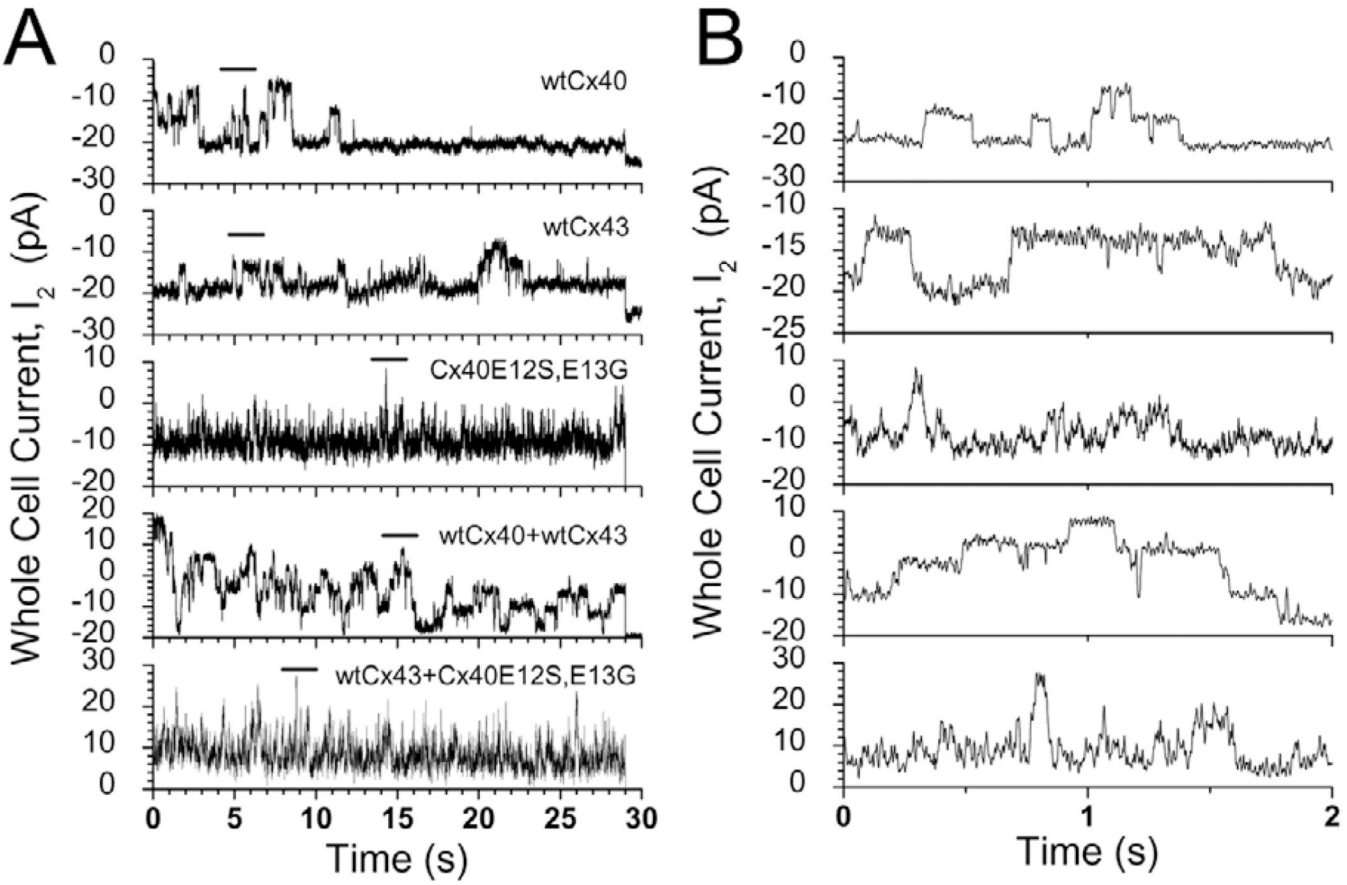

Fig. 6.

Single gap junction channel events detected in whole-cell two-current recordings obtained from N2a cells expressing different connexins (during a 30-second V_j pulse of −40 mV): wild-type Cx40 (stably, top trace), wild-type Cx43 (stably, second trace), Cx40E12S,E13G (transiently, third trace), wild-type Cx43 (stably) co-expressed with wild-type Cx40 (transiently, fourth trace), and wild-type Cx43 (stably) co-expressed with Cx40E12S,E13G (transiently, fifth trace). Panels A and B show channel events on different time scales. Panel B shows a 2-seconds excerpt (indicated with a bar above each trace in panel A) displayed at an expanded time scale to illustrate single channel events more clearly.

NIH-PA Author Manuscript
NIH-PA Author Manuscript
NIH-PA Author Manuscript

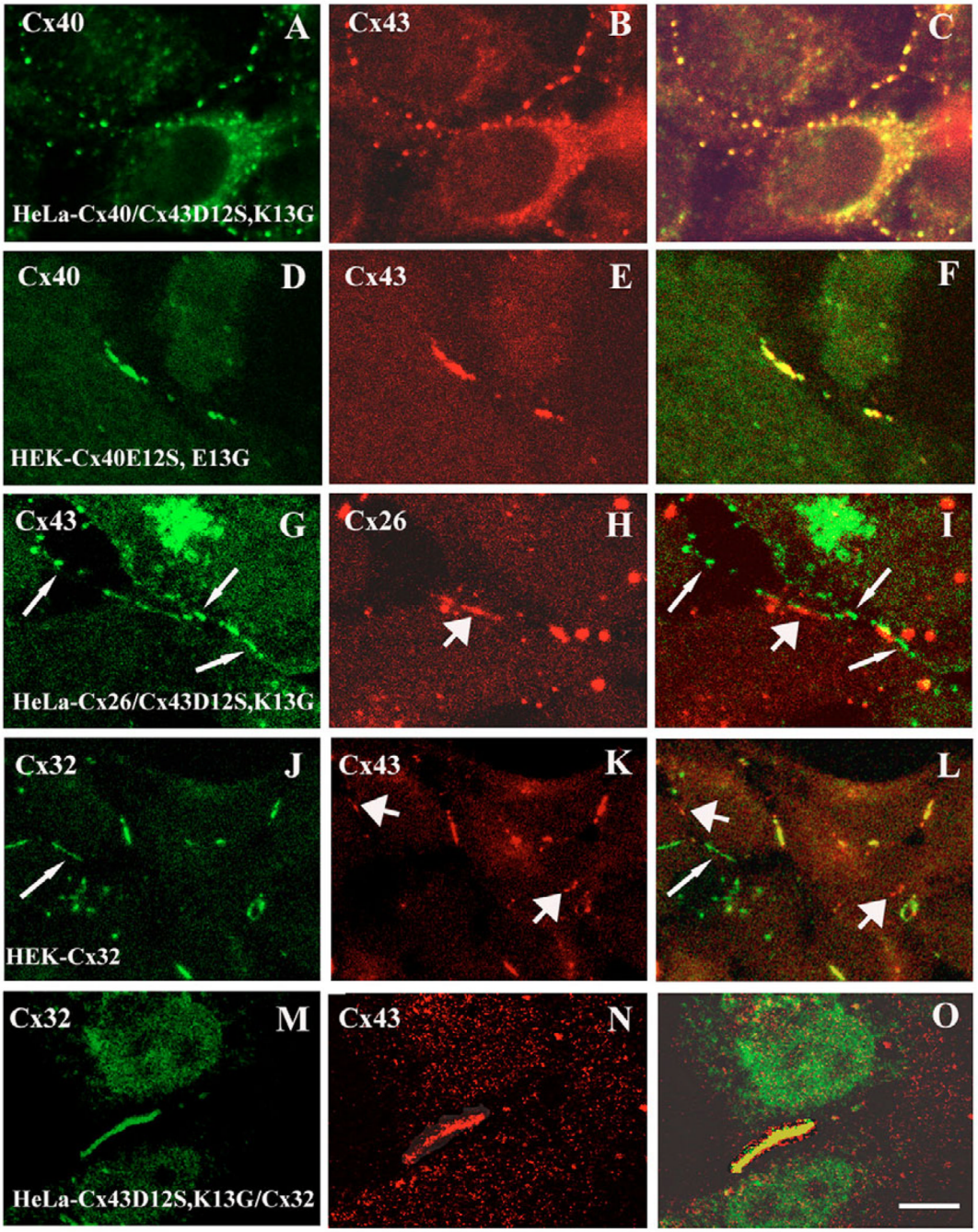

Fig. 7.

Double-label immunolocalization of mutant and wild-type connexins. All panels show stably transfected cells, except M–O, where Cx32 was introduced transiently to make HeLa-Cx43D12S,K13G/Cx32 cells. Individual immunoreactive connexins are detected in the first two columns and appear green or red. Merged images are shown in the right panels where overlap appears yellow. Arrows indicate examples of non-overlapping staining for only a single connexin (long, thin arrows: green only; heavy arrows: red only). (A–C) Fluorescence micrographs of HeLa-Cx40/Cx43D12S,K13G cells showing immunoreactive Cx40 in green (A), Cx43 in red (B) and the overlap of both immunoreactivities (C). Wild-type Cx40 and Cx43D12S,K13G perfectly co-localize. (D–F) Fluorescence micrographs of HEK-

NIH-PA Author Manuscript

NIH-PA Author Manuscript

NIH-PA Author Manuscript

Cx40E12S, E13G cells showing immunoreactive Cx40 in green (D), Cx43 in red (E) and the overlap of both immunoreactivities (F). Wild-type Cx43 and Cx40E12S,E13G perfectly co-localize. (H–I) Fluorescence micrographs of HeLa-Cx26/Cx43D12S,K13G cells showing immunoreactive Cx43 in green (G), Cx26 in red (H) and the merged image of both immunoreactivities (I). Wild-type Cx26 and Cx43D12S,K13G do not co-localize. (J–L) Immunofluorescence images of HEK-Cx32 cells showing immunoreactive Cx32 in green (J), Cx43 in red (K) and the merged image of both immunoreactivities (L). Wild-type Cx32 and Cx43 rarely co-localize. (M–O) Immunofluorescence images of HeLa-Cx43D12S,K13G/Cx32 cells showing immunoreactive Cx32 in green (M), Cx43 in red (N) and the merged image of both immunoreactivities (O). Wild-type Cx32 and Cx43D12S,K13G extensively co-localize. Bar, 8 μm for A–C, 6 μm for G–I, 5 μm for D–F and M–O, 4 μm for J–L.

NIH-PA Author Manuscript
NIH-PA Author Manuscript
NIH-PA Author Manuscript

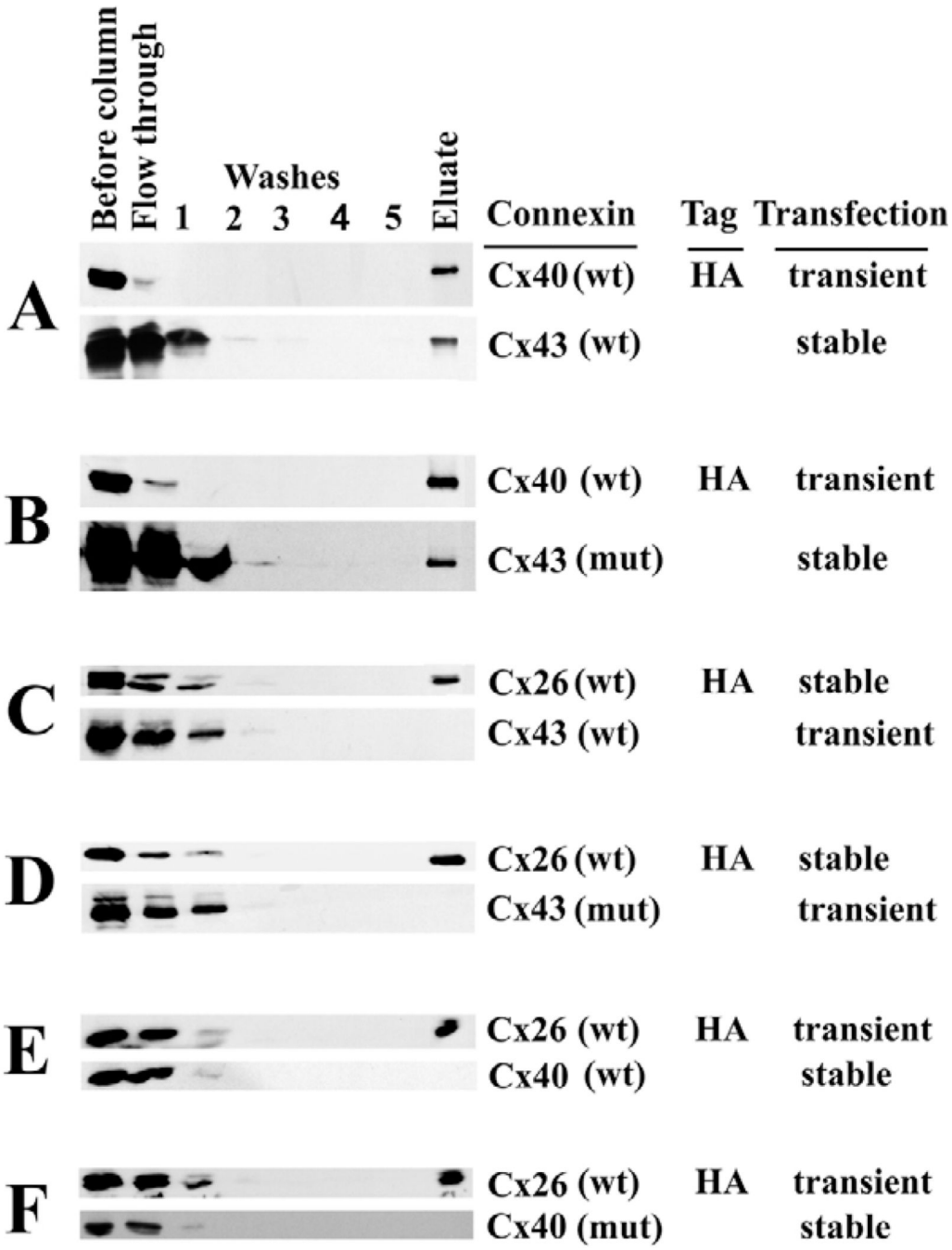

Fig. 8.

Affinity purification of HA-tagged connexin and potentially associated proteins. The presence and abundance of Cx40, Cx43 or Cx26 were detected in the cell extract, washes and eluted material by immunoblotting using anti-connexin antibodies. Gels were loaded with 25 μg of protein (corresponding to 1/10 of the amount incubated with MicroBeads) in the lane labeled ‘Before column’; 1/10 of the fraction collected as a ‘Flow through’, 1/5 of each of the ‘Washes’; and 1/10 of the ‘Eluate’ (corresponding to 25 μg of protein applied to the purification column). (A) Purification of proteins from HeLa-Cx43 cells transfected with Cx40HA. (B) Purification of proteins from HeLa-Cx43D12S,K13G [Cx43 (mut)] cells transfected with Cx40HA. (C) Purification of proteins from HeLa-Cx26HA cells transfected

with Cx43. (D) Purification of proteins from HeLa-Cx26HA cells transfected with Cx43D12S,K13G. (E) Purification of proteins from HeLa-Cx40 cells transfected with Cx26HA. (F) Purification of proteins from HeLa-Cx40E12S,E13G [Cx40 (mut)] cells transfected with Cx26HA.

NIH-PA Author Manuscript
NIH-PA Author Manuscript
NIH-PA Author Manuscript

NIH-PA Author Manuscript
NIH-PA Author Manuscript
NIH-PA Author Manuscript

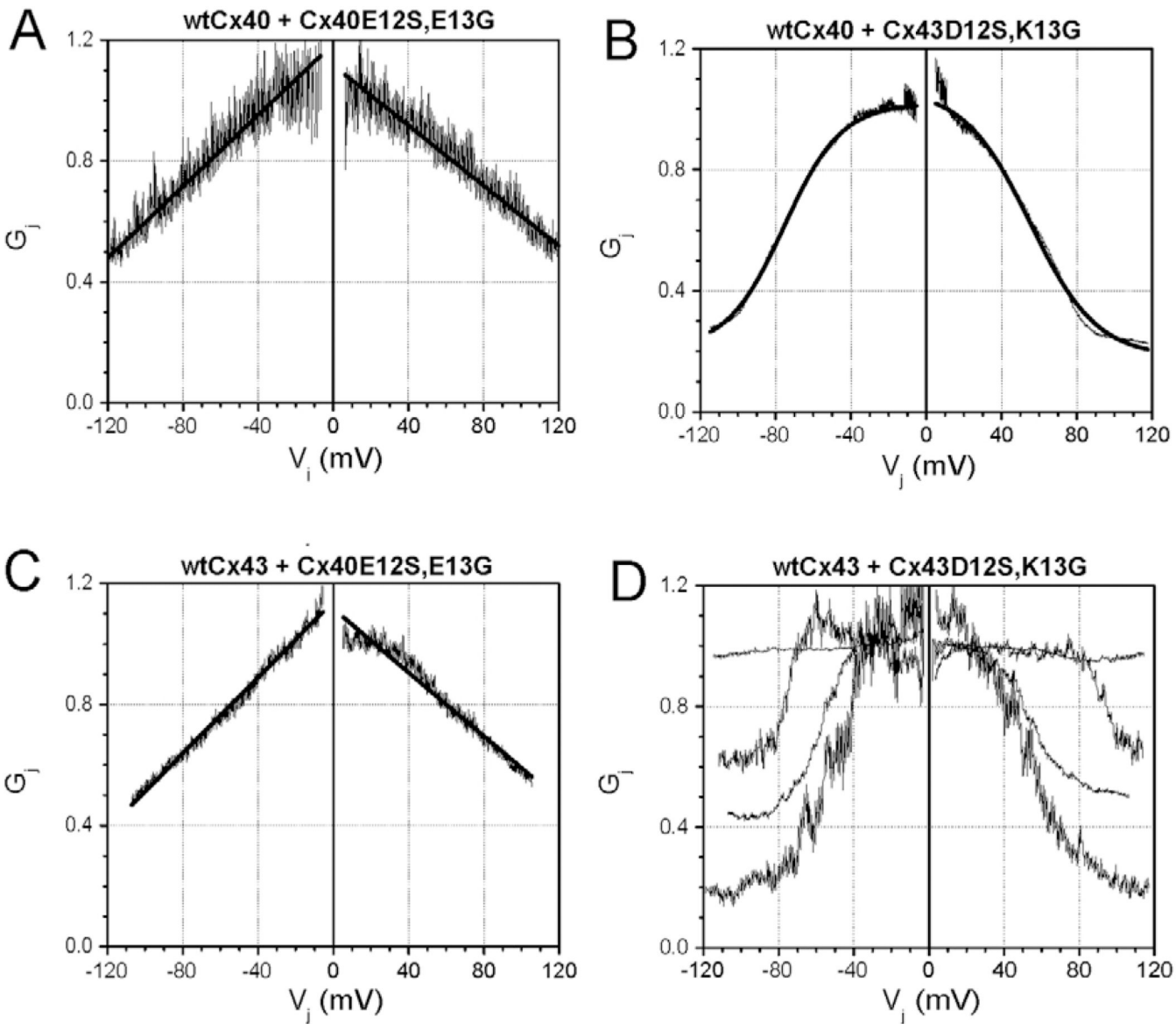

Fig. 9.

Steady-state G_j-V_j relationships in pairs of cells co-expressing a wild-type and a mutant connexin. (A) N2a-Cx40 cells transfected with Cx40E12S,E13G. (B) N2a-Cx40 cells transfected with Cx43D12S,K13G. (C) N2a-Cx43 cells transfected with Cx40E12S,E13G. (D) N2a-Cx43 cells transfected with Cx43D12S,K13G. In all experiments, the first connexin was stably transfected, and the second was introduced transiently. The mathematical fits to the G_j-V_j relationships in panels A–C are provided in Tables 2 and 3.

NIH-PA Author Manuscript

NIH-PA Author Manuscript

NIH-PA Author Manuscript

Table 1

Lucifer Yellow transfer in HeLa cells stably transfected with wild-type or mutant connexins

Cell line	Dye-filled neighbors (mean ± s.e.m.)	Number of injections (*n*)	Injections showing dye transfer (%)
HeLa-Cx43	8.00±0.92	16	100
HeLa-Cx43D12S,K12G	3.60±0.16*	47	100
HeLa-Cx40	1.73±0.26	41	69
HeLa-Cx40E12S,E12G	2.40±0.32†	10	100
HeLa-Cx40/Cx43	3.90±0.35	51	86
HeLa-Cx40/Cx43D12S,K12G	3.23±0.36†	13	100

The results of individual experiments for wild-type connexin were compared with the results obtained from corresponding mutants; the significance of differences was evaluated using Student's *t* test. The number of dye-filled neighbors was reduced as compared with HeLaCx43 (*P<0.001). Transfer among HeLaCx40E12S,E12G or HeLaCx40/Cx43D12S,K12G cells was not statistically different from that among HeLaCx40 or HeLaCx40/Cx43 cells, respectively (†P>0.2).

NIH-PA Author Manuscript NIH-PA Author Manuscript NIH-PA Author Manuscript

Table 2

Values for the Boltzmann equation fits of the steady-state G_j-V_j curves

Cell#1 **Cell#2**	**wtCx40** **wtCx40**		**Cx40E12S,E13G** **wtCx40**		**wtCx43** **wtCx43**		**Cx43D12S,K13G** **wtCx43***		**Cx43D12S,K13G/wtCx40** **Cx43D12S,K13G/wtCx40**	
	$-V_j$	$+V_j$	$-V_j$	$+V_j$	$-V_j$	$+V_j$	$-V_j$	$+V_j$	$-V_j$	$+V_j$
G_{max}	1.02±0.02	0.98±0.1	1.45±0.01	1.50±0.01	1.06±0.001	0.96±0.002	1.12±0.001	1.12±0.002	1.02±0.001	1.07±0.003
$V_{½}$ (mV)	−49.9±0.1	50.5±0.1	−55.6±0.9	+45.6±0.5	−58.5±0.1	+67.3±0.2	−76.5±0.2	+19.1±0.2	−75.5±0.1	55.3±0.2
z	−3.68±0.04	+3.13±0.04	−3.84±0.47	+1.05±0.03	−2.70±0.02	+2.22±0.04	−5.08±0.16	+1.31±0.01	−1.67±0.01	+1.43±0.02
G_{min}	0.14±0.001	0.19±0.002	1.23±0.004	0.03±0.01	0.19±0.001	0.19±0.003	0.88±0.002	0.02±0.002	0.21±0.003	0.18±0.003
n	5		4		4		4		6	
r	0.95	0.95	0.95	0.92	0.97	0.95	0.98	0.96	0.98	0.97

*Stably transfected HeLa-Cx43D12S,K13G and Hela-Cx43 cells were used for this heterotypic combination. All G_j-V_j relationships were fit with the Boltzmann equation:

$$G_j^{ss} = \left\langle \frac{G_{ss}^{max} \bullet \{\exp[A \bullet (V_j - V_{\frac{1}{2}})]\} + G_{ss}^{min}}{1 + \{\exp[A \bullet (V_j - V_{\frac{1}{2}})]\}} \right\rangle,$$

where $G_{ss}^{max} = 1$ ($G_j = g_j/g_{j,\,max}$) = resting normalized slope conductance between ±5 and ±20 mV for each experiment; G_{ss}^{min} = minimum value of $g_j/g_{j,\,max}$; A = slope factor (=zF/RT at 20°C); and $V_{1/2}$= half-inactivation voltage. n, number of experiments; r, correlation coefficient.

NIH-PA Author Manuscript
NIH-PA Author Manuscript
NIH-PA Author Manuscript

Table 3

Values for the linear fits of G_j-V_j curves

Cell#1 **Cell#2**	**Cx40E12S,E12G** **Cx40E12S,E12G**		**Cx43D12S,K12G** **Cx43D12S,K12G**		**Cx40E12S,E12G/wtCx40** **Cx40E12S,E12G/wtCx40**		**Cx40E12S,E12G/wtCx43** **Cx40E12S,E12G/wtCx43**	
	$-V_j$	$+V_j$	$-V_j$	$+V_j$	$-V_j$	$+V_j$	$-V_j$	$+V$
G_{max}	1.12±0.004	1.16±0.004	1.00±0.004	1.05±0.004	1.19±0.003	1.12±0.003	1.14±0.004	1.12±0.004
Slope (mV^{-1})	0.0049±0.0001	−0.0057±0.0001	0.0006±0.0001	−0.0013±0.0001	0.0059±0.0001	−0.0050±0.0001	0.0063±0.0001	−0.0053±0.0001
n	6		4		7		5	
r	0.95	0.96	0.99	0.99	0.92	0.94	0.97	0.96

All G_j-V_j relationships were fit with the linear equation G_j = slope × V_j + G_{max}. *n*, number of experiments; *r*, correlation coefficient.